Fluorescence and Theoretical Calculation of Phenylhydrazone Derivatives and Fluorine Boron Complex: Synthesis and Fluorescence Characteristics

[1]Ping Tang, [1]Luping Lyu* and [2]Yujin Li
[1]*Linjiang College, Hangzhou Vocational and Technical College, Hangzhou 310018, People's Republic of China.*
[2]*College of Chemical Engineering, Zhejiang University of Technology, Hangzhou 310014, People's Republic of China.*
mailofllp@126.com*

(Received on 7th February 2018, accepted in revised form 29th March 2019)

Summary: A sereis of phenylhydrazone-based derivatives and their corresponding BF_2 complexes were synthesized efficiently by a three-step reaction. Photophysical performance was investigated in different organic solvents and in the solid state. Although these compounds exhibited feeble fluorescent intensity in solution-state, BF_2 complexes showed weaker fluorescence in solid state compared to precursors **2**, which were caused by slight geometry relaxation of upon photo excitation. Density Functional Theory calculations was carried out to confirm above inference**.**

Keywords: Boron Complexes; Solid State; Fluorescence; DFT Calculation.

Introduction

phenylhydrazone-based compounds have been reported in the field of academic research and broadly applied to aggregation-induced emission enhancement [1], fluorescent molecular probes [2, 3], electroluminescence [4], photodynamic therapy [5], anticathepsin agents [6], Organocatalytic [7, 8], nonlinear optical material [9], determination of Cu(II), Zn(II) and Mn(II) [10], acetate ion recognition [11, 12], etc. Meanwhile, their corresponding BF_2 complexes have been extensively known as fluorescent dyes which have exhibited practical applications in electrochromic display systems [13, 14], solar cells [15, 16], liquid crystals [17, 18] and optical storage devices [19, 20]. In 2015 Li's group reported a series of phenylhydrazone derivatives and their corresponding BF_2 complexes indicating robust aggregation-induced emission enhancement properties and high solid-state fluorescent intensity following a huge Stokes Shift [1, 21]. This research supported us to create a new range of phenylhydrazone-based derivatives and their corresponding BF_2 complexes and to investigate other novel optical characters.

Hence, a new series of phenylhydrazone-based derivatives and their corresponding BF_2 complexes were designed and synthesized. The compounds demonstrated an attractive fluorescence characters in the solid states. Herein, we describe the synthesis and optical properties of these compounds. In addition, Density Functional Theory(DFT) and time-dependent DFT(TD-DFT) calculations were carried out to confirm the experimental results.

Experimental

Materials and methods

In the present research, unless otherwise noted, all the chemicals were used with no purification and were purchased from commercial enterprises. Standard methods were used to purify all the solvents prior to use. Melting points (m. p.) were carried on a X-4 electro-thermal digital melting point apparatus. Nuclear magnetic resonance (^1H and ^{13}C NMR) spectra were run on a Bruker AM 500 spectrometer (Bruker) with chemical shifts reported as ppm at 500 and 125 MHz, respectively, (in $CDCl_3$ as internal standard).

Fluorescence spectra were obtained on a F-7000 Fluorescence spectrophotometer. The emission was measured in the steady state mode by exciting at the λ_{max} (lower energy MLCT band) for each compound with exit and entrance slits set at 5 nm. Fluorescence spectra were recorded for 3 times and average values of the integrated areas of fluorescence were adopted to calculate Φ_f in solution. It can be used for photochemical checking at spectroscopic grade. On a UV-2550, absorption spectra of UV-Vis were measured. The Φ_f values in solution were determined by using a common method. In this method, quinine sulfate (Φ = 0.55 in 0.05 M H_2SO_4 solution) was

*To whom all correspondence should be addressed.

treated as a standard and dilute solutions of the mixtures were used in organic dissolvent($1\cdot10^{-5}$ $mol\cdot L^{-1}$).

Density Functional Theory (DFT) and time-dependent DFT (TD-DFT) calculation with 6-31G/B3LYP level have been perfomed to optimize all the structures. All the calculations were carried out on Gaussian 09W program package [22, 23].

Synthesis

General synthesis procedure of 2a-2c. Under nitrogen atmosphere, 2,4-Dihydroxyacetophenone (10 mmol), methyl hydrazinecarboxylate 0.74g (10 mmol) were dissolved in stirred methanol (15 ml) and left for 2.5 h at room temperature. The resulting solid was filtered off and recrystallized from ethanol for three times to give the title compounds 1.95 g **2a**, 1.77g **2b**, 1.69 g **2c.**

(E)-Methyl N'-[1-(4-hydroxyphenyl)ethylidene]hydrazinecarboxylate (**2a**) White solid. Yield, 87.1%. M.P.: 208-212 °C. ^{1}H-NMR (500 MHz, $CDCl_3$) δ(ppm): 13.04 (s, 1H), 10.59 (s, 1H), 9.72 (s, 1H), 7.33 (d, J = 8.7 Hz, 1H), 6.29 (dd, J = 8.7, 2.4 Hz, 1H), 6.23 (d, J = 2.4 Hz, 1H), 3.74 (s, 3H), 2.23 (s, 3H); HRMS (ESI) m/z calcd for: $C_{10}H_{13}N_2O_4^+(M+H)^+$ 225.0869, found 225.0869.

*(E)-Methyl N'-(2,4-dihydroxybenzylidene)hydrazinecarboxylate (**2b**)* White solid. Yield, 84.3%. M.P.: 109-113 °C; ^{1}H-NMR (500 MHz, $CDCl_3$) δ(ppm): 11.07 (d, J = 42.9 Hz, 2H), 9.81 (s, 1H), 8.10 (s, 1H), 7.20 (dd, J = 8.3, 2.8 Hz, 1H), 6.44-6.20 (m, 2H), 3.69 (s, 3H); HRMS (ESI) m/z calcd for $C_9H_{11}N_2O_4^+(M+H)^+$ 211.0713, found 211.0713.

*(E)-Methyl N'-(4-methyoxybenzylidene) hydrazinecarboxylate (**2c**)* White solid. Yield, 81.3%. M.P.: 140-142 °C. ^{1}H-NMR (500 MHz, $CDCl_3$) δ(ppm): 12.45 (s, 1H), 7.43 (d, J = 7.7 Hz, 1H), 7.29 (dd, J = 9.1, 2.1 Hz, 1H), 7.00 (dd, J = 8.2, 1.1 Hz, 1H), 6.93-6.84 (m, 1H), 3.91 (s, 3H), 2.30 (s, 3H); HRMS (ESI) m/z calcd for $C_{10}H_{13}N_2O_3^+(M+H)^+$209.0921, found209.0921.

General synthesis procedure of 3a-3b. Under nitrogen atmosphere, to a solvent of 0.20 g **2a** in toluene(10 mL), 0.7 ml(4.0 mmol)N,N-diisopropyl ethylamine was put into drop by drop within 10 min.Then 0.5 ml(4.0 mmol) Boron trifluoride diethyl etherate was slowly added into above mixture and refluxed for 4 hours. Then the reaction mixture was concentrated to product crude product under reduced pressure. Silica gel chromatography eluting (silica gel, ethyl acetate: petroleum ether = 1:1) was used to purify the crude product causing 80 mg **2a**, and 95 mg **2b**, as yellow solid.

*methyl (2,2-difluoro-7-hydroxy-4-methyl-2H-2l4,3l4-benzo[e][1,3,2]oxazaborinin-3-yl)carbamate (**3a**)* Yellow solid. Yield, 71.0%. M.P.: 233-235 °C. ^{1}H-NMR (500 MHz, $CDCl_3$) δ(ppm): 8.72 (s, 1H), 7.36 (d, J = 8.6 Hz, 1H), 6.35 (dd, J = 8.5, 2.2 Hz, 1H), 6.29 (d, J = 2.1 Hz, 1H), 4.03 (d, J = 7.1 Hz, 1H), 3.44 (d, J = 7.0 Hz, 3H), 2.51 (s, 3H); ^{13}C NMR (125 MHz, $CDCl_3$) δ(ppm): 161.27, 160.84, 155.32, 152.61, 130.79, 111.22, 107.90, 104.01, 51.3, 17.65; HRMS (ESI) m/z calcd for $C_{10}H_{12}BF_2N_2O_4^+(M+H)^+$ 273.0853, found 273.0867.

*methyl (2,2-difluoro-7-hydroxy-2H-2l4,3l4-benzo[e][1,3,2]oxazaborinin-3-yl)carbamate (**3b**)* Yellow solid. Yield, 82.1%, M.P.:217-218°C. ^{1}H-NMR (500 MHz, $CDCl_3$) δ(ppm): 8.61 (s, 1H), 8.21 (s, 1H), 7.29 (d, J = 8.5 Hz, 1H), 6.31 (dd, J = 8.6, 2.2 Hz, 1H), 6.27 (d, J = 2.3 Hz, 1H), 4.12 (d, J = 7.0 Hz, 1H), 3.41 (d, J = 6.9 Hz, 3H); ^{13}C NMR (125 MHz, $CDCl_3$) δ(ppm): 162.31, 161.97, 154.12, 153.72, 131.81, 110.12, 108.62, 103.21, 51.3; HRMS (ESI) m/z calcd for $C_9H_{10}BF_2N_2O_4^+(M+H)^+$ 259.0648, found 259.0676.

Results and Discussion

Synthesis

Scheme-1 shows the preparation for the substituted phenylhydrazone derivatives (precursor **2**) and their corresponding boron complexes (BODIHY **3**): **2a**, **2b**, **2c**, **3a and 3b.** First, mixture of dimethyl carbonate and hydrazine hydrate was refluxed for 7 hours to obtain methyl hydrazinecarboxylate **1** (1.5equiv). Then phenylhydrazone derivatives **2** were accomplished by condensation with aromatic aldehydes (ketones) and methyl hydrazinecarboxylate (1.0equiv) in CH_3OH at room temperature. Finally, phenylhydrazone derivatives and an excess of $BF_3.Et_2O$ in DCM with N,N-Diisopropyl ethylamine as the base gave BODIHY **3** with a yield of 71.0 % (**3a**) and 82.1% (**3b**). BODIHY **3** were purified by column chromatography (silica gel, EA:PE = 1:1). All the structures were sufficiently characterized by ^{13}C-NMR, ^{1}H-NMR, GC-MS and HRMS analysis (Table-1).

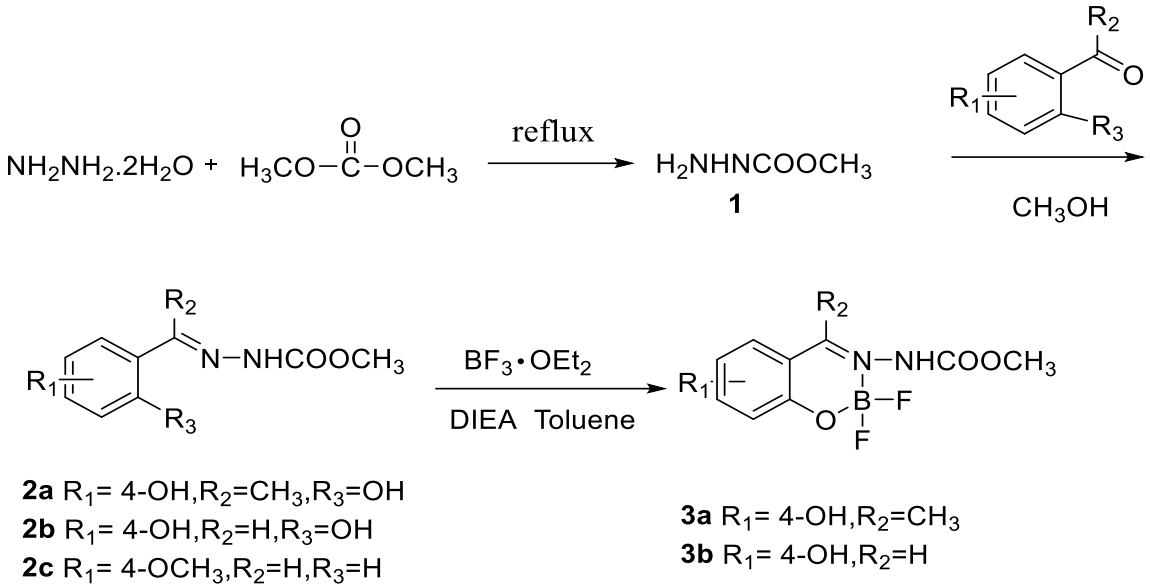

Scheme-1: Synthesis of compounds **2a**, **2b**, **2c**, **3a**, **3b**.

Table-1: Structures of compounds 2a, 2b, 2c, 3a, 3b.

compound	R^1	R^2	R^3
2a	**4-OH**	**CH_3**	**OH**
2b	**4-OH**	**H**	**OH**
2c	**4-OCH_3**	**H**	**H**
3a	**4-OH**	**CH_3**	
3b	**4-OH**	**H**	

UV-Vis spectra and emission spectra of 2c in solution

The final products **2a**, **2b**, **2c**, **3a** and **3b** demonstrated considerable stability and solubility in solvents like CH_3CN, EtOH, DCM, DMF, THF, EA and Chloroform. No overt and apparent fluorescence and color fading were found in months using rigorous examination. Precursor **2c**'s solvent effect on absorption and fluorescence properties was tested (Table-2 and Fig. 1). As show in Fig. 1 and Table-2, precursor 2c exhibited a sharp absorption peak at approximately 320 nm. The maximum absorption wavelength (λ_{max}) of BODIHY **3** (368 nm) showed more bathochromic than the precursor **2c**. Furthermore, it was obvious that the dissolvent polarity imposed slight effect on **2c**'s maximum absorption wavelength (λ_{max}), which indicated that the dipole moments of the molecules in both excited and ground states were more or less equal [24]. Meanwhile, it was found that the maximum fluorescence intensity of precursor **2c** was reached in THF which is the best solvent and was highly dependent on solvents. Precursor **2c** displayed a strongest fluorescence intensity (λ_{em}=352 nm) with 180 fluorescence intensity (signal response value) in THF, but the value was lower than 40 in DCM (Fig. 1). As a result, the fluorescence quantum yields (Φ_f) of Precursor **2c** were below 0.01 in DCM. It hardly exhibited fluorescence in DCM. In Addition, maximum emission wavelength of **2c** underwent a slight change in different organic solvents.

UV-Vis spectra and emission spectra of **2a-3b** *in solution*

Optical data of compounds **2a-3b** in THF was measured respectively to examine the substituent group effects (Table-2). As shown in Table-2 and Fig. 2, compounds **2a-3b'**s maximum absorption wavelength (λ_{abs}) were at about 317 nm, 317 nm, 317 nm, 367 nm and 360 nm, respectively. Precursors **2a**, **2b** and **2c** exhibited almost the same absorption patterns with highest absorption peaks at 317 nm. The result also showed that it had rarely effect on the maximum absorption peak of precursors **2** under different substituents on benzene ring. BODIHY **3a** displayed a slight bathochromic shift of around 7 nm compared with **3b** because of the electron-donating effect of methyl. BODIHY **3a**(367 nm) and **3b**(360 nm) demonstrated an obvious bathochromic shift (43-50 nm) compared with the corresponding precursor **2a**(317 nm) and **2b**(317 nm) (Table-1). The complexation of BF_2 increased the molecular rigidity and coplanarity of BODIHY **3**, which caused the bathochromic shift.

Table-2: Photophysical properties for compounds **2a**, **2b**, **2c**, **3a**, **3b**.

Compounds	Matrix	å($M^{-1}cm^{-1}$)	$ë_{abs}$(max) （nm)	$ë_{em}$(max) （nm)	Stokes Shift(nm)	Öf
2a	THF	10700	317	374	57	0.05
	solid		318	471	153	/
2b	THF	6900	317	374	57	0.05
	solid		320	473	153	/
2c	DCM	2100	321	354	33	0.01
	CHCl3	7700	318	349	31	0.03
	EA	2900	318	351	33	0.06
	EtOH	4300	319	350	31	0.05
	MeCN	3900	320	348	28	0.06
	THF	6200	317	352	35	0.08
	DMF	6200	318	351	33	0.07
	solid		320	521	201	0.20
3a	DCM	50400	368	412	45	0.01
	CHCl3	56500	369	413	44	0.16
	EA	42900	365	403	39	0.15
	EtOH	44500	367	508	142	/
	MeCN	52200	364	410	47	/
	THF	55000	367	404	37	0.21
	DMF	53400	368	413	46	/
	solid		418	508	90	/
3b	THF	54000	360	399	39	0.19

Fluorescence quantum yields were measured with quinine sulfate (Φ_f=54.6% in 0.05 M H_2SO_4) as the reference

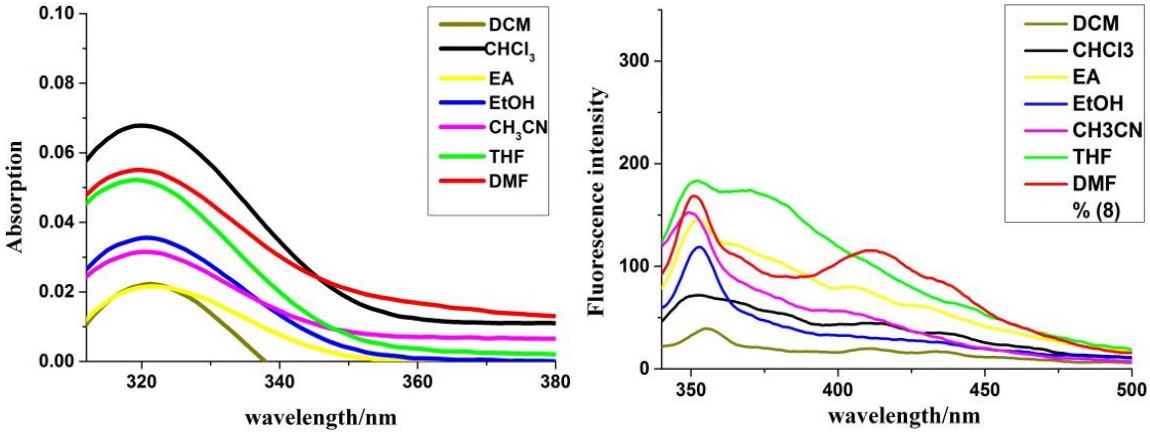

Fig. 1: Left: Absorption spectrum of compound **2c** (1×10^{-5} mol·L^{-1}) in different solvents. Right: Emission spectrum of compound **2c** (1×10^{-5} mol·L^{-1}) in different solvents (PMT Voltage: 700 V).

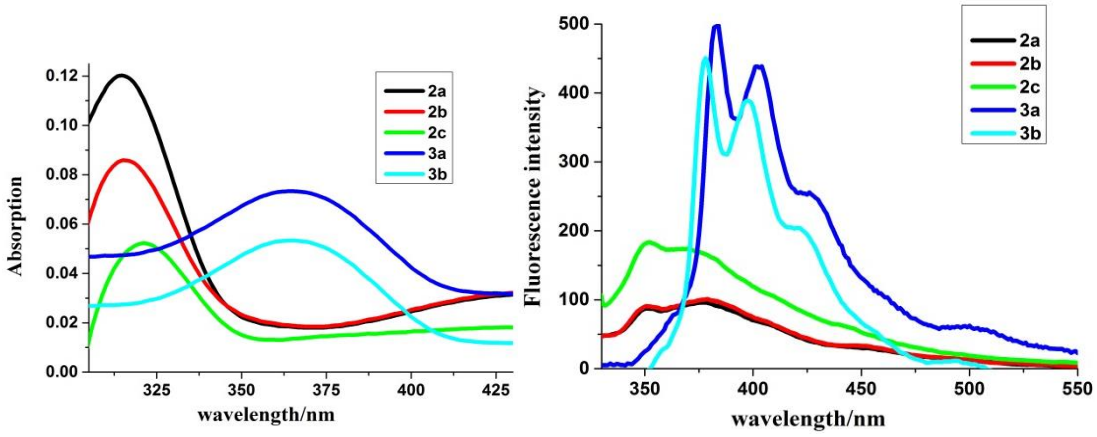

Fig. 2: Left: Absorption spectrum of compounds **2a**, **2b**, **2c**, **3a**, **3b** (1×10^{-5} mol·L^{-1}) in THF. Right: Emission spectrum of compounds **2a**, **2b**, **2c**, **3a**, **3b** (1×10^{-5} mol·L^{-1}) in THF (PMT Voltage: 700 V).

As detailed in Table-2 and Fig. 2, compounds **2a-3b** possessed the Stokes Shifts between 35-57 nm in THF. Of all, compounds **2a** and **2b** was the two with the highest Stokes Shift (57 nm) with emission at 374 nm and excitation at 317 nm. Compared with **2c**, precursors **2a** and **2b** (with hydroxyl on benzene) emerged the larger Stokes Shifts and longer wavelengths in the fluorescence emission spectra because the electron donating hydroxyl on benzene helped the **2a** and **2b**'s expansion of Stokes Shifts. Similarly, the fluorescence emission wavelength of **3a** (404 nm) was larger than **3b** (399 nm) due to the presence of electron donating methyl group of **3a**. All the compounds showed a blue fluorescence, but fluorescence intensity of BODIHY **3** was much higher than precursor **2**a-**2c**. Correspondingly, compound precursors **2**a-**2c** were observed to have lower quantum yield with 5%(**2**a), 5%(**2b**) and 8% (**2c)** than **3a**(21%) and **3b**(19%).

Emission spectra of 3a-2b in solid state

Further, fluorescence Emission spectra of all compounds in the solid states were tested (Table-2). The color of compounds **2a-3b** in their solid state by direct visualization and UV lamp (365 nm) were shown in Fig. 3. As reflected in Table-2 and Fig. 3, both precursor **2** and BODIHY **3** had the large Stokes shifts between about 90 nm and 201 nm in the solid-state. The maximum Stokes shift of **2c** was up to 201 nm, with excitation at 320 nm and emission at 521 nm in the solid-state. The fluorescence intensity of BODIHY **3** was obviously lower than the corresponding precursor **2**. Precursor **2a-2c** looked bright blue under the excitation of UV light. However, BODIHY **3a** and **3b** hardly exhibited fluorescence in their solid state. This phenomenon could be ascribed to their high coplanarity which resulted in piling of molecules and strong intermolecular interactions, correspondingly leading to concentration quenching in the solid state [22, 23]. On the other hand, precursor **2a-2c** exhibited a solid-state emission partially due to their more twisted molecular structure preventing the compact packing of molecules [22, 23]. As reflected in Table-2, solid-state emissions spectra reached to a 471 nm - 508 nm ranges and were bathochromic-shifted compared with their respective emissions in solution. Furthermore, relative to **2a** and **2b**, precursor **2a-2c**'s maximum emission spectrum was more bathochromic-shifted. Which might be possibly due to the π-π stacking and denser aggregation of molecules in the solid state [25].

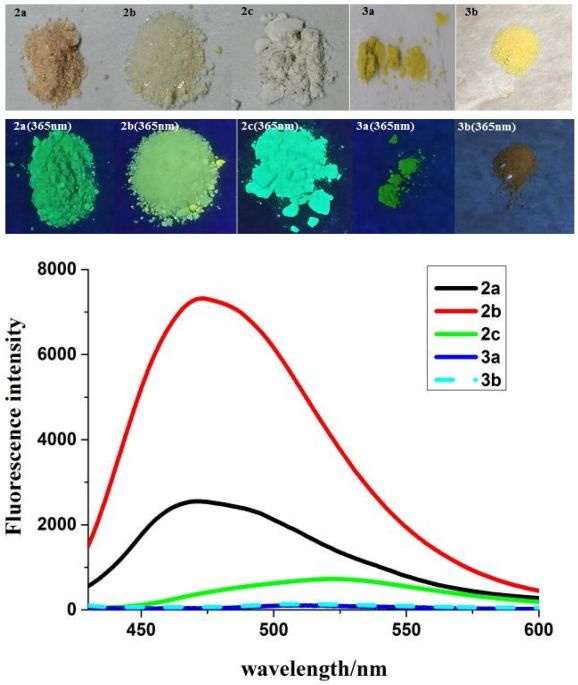

Fig. 3: Left: The color of compounds **2a**, **2b**, **2c**, **3a**, **3b** in solid state under visible light (upper row) and UV lamp (365 nm, lower row). Right: The emission spectra of compounds **2a**, **2b**, **2c**, **3a**, **3b** in the solid state (PMT Voltage: 700 V).

Quantum chemical calculations: rationalize the excitation and emission spectra

To better comprehend photophysical properties of the precursor **2** and the BODIHY **3**, such as the UV-vis absorption and fluorescence, BODIHY **3a**'s geometry at the S_0 state and the S_1 state was optimized by Density Functional Theory (DFT) Quantum calculations at the B3LYP/6-31G level, which was performed in Gaussian 09W class of programs[24, 25]. The optimized configuration of BODIHY **3a** was illustrated in Fig. 5. It was found that both of the optimized configurations at S_0 state and the S_1 state adopted chair structure. The dihedral angles between phenyl ring and BODIHY core of S_0 state and S_1 state were 8.67° and 9.12°, respectively. Which indicated that coplanarity of S_0 state was sight better than that of S_1 state (Fig. 5)? The geometry of the S_1 excited state, which is responsible for the fluorescence (Kasha's rule) [26], is more or less same as S_0 state geometry (Fig.5). This can explain why BODIHY **3a**

and **3b** hardly exhibited fluorescence in solid state. As shown in Fig. 4, the energy gap between the HOMO and LUMO of the BODIHY **3a** was 3.38 eV. In addition, the calculated absorption and emission peaks of the **3a** were located at 334 nm and 414 nm, respectively, which were consistent with the experimental results of 368 nm and 413 nm.

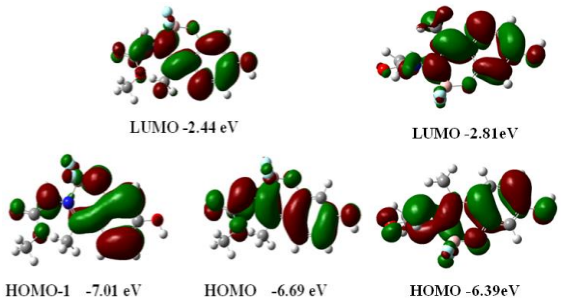

Fig. 4: Molecular orbital amplitude plots of HOMO and LUMO energy levels and Optimized geometries of 3a in S_0 (left) and S_1 (right).

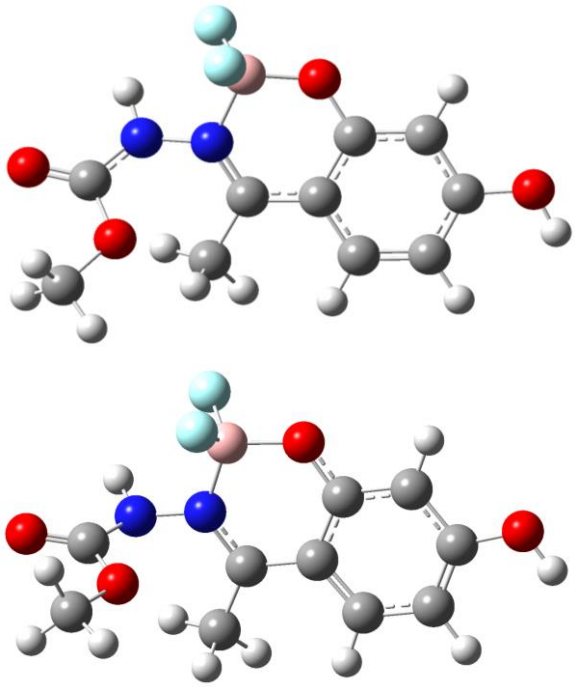

Fig. 5: Optimized geometry of the compound 3a in the solid state in S_o (Left) and S_1(Right).

Conclusion

In conclusion, a series of phenylhydrazone-based derivatives and their corresponding BF_2 complexes were developed using readily procedures under mild conditions. All the compounds exhibited visible fluorescence in their solutions. However, precursors **2** showed much more enhanced fluorescence in solid state compared to corresponding BF_2 complexes. The geometries of the molecules at the S_0 state and the S_1 excited state were optimized by DFT and TD-DFT, respectively. The results of the calculation of the UV--vis absorption and emission were in agreement with the experimental results. The small geometry relaxation was proposed to the main cause for the weak fluorescence of BODIHY 3a in solid state.

Acknowledgments

We gratefully acknowledge the financial support of Hangzhou agricultural scientific research project(20160432B25, 20180432B35), College Students in Zhejiang Province Sciences and Technology Innovation Activities Plan & Xinmiao Talents Program (No.2017R452002) and China Scholarship Council(File No.201708330572), Zhejiang Public Welfare Technology Research Program (LGN19C200014), zhejiang Philosophy and Social Science Planning Project (20NDJC337YBM) .

References

1. J. Zheng, F. Huang , Y. Li , T. Xu , H. Xu , J. Jia , Q. Ye , J. Gao, The aggregation-induced emission enhancement properties of BF_2 complex isatin-phenylhydrazone: Synthesis and fluorescence characteristics, *Dyes and Pigments*, **113**, 502 (2015).
2. L. Zang, C. Liang, Y. Wang, W. Bu, H. Sun, S. Jiang, A highly specific pyrene-based fluorescent probe for hypochlorite and its application in cell imaging, *Sensor Actuat B-Chem*, **211**, 164 (2015).
3. W.Huang, H. Su, S, Yao, Z. Yang, H, Lin, H. Lin, A Simple and Neutral Receptor Acting as a Sensitive and Switch-on Fluorescent Chemosensor for $H_2PO_4^-$, *J. Lumin.*, **131**, 1913 (2011).
4. A. C. Jones, Development s in metalorganic precursors for semiconductor growth from the vapour phase, *Chem. Soc. Rev.* **26**, 101 (1997).
5. J. Cheng, W. Li, G. Tan, Z. Wang, S. Li, Y. Jin, Synthesis and in vitro photodynamic therapy of chlorin derivative 131-ortho-trifluoromethyl-phenylhydrazone modified pyropheophorbide-a, *Biomed. Pharmacother.*, **87**, 263 (2017).

6. N. Raghav, M. Singh. SAR studies of some acetophenone phenylhydrazone based pyrazole derivatives as anticathepsin agents, *Bioorg. Chem.*, **75**, 38-49(2017).
7. W. Dai, H. Lu, X. L. Jiang, T. T. Gao, F. Shi, Organocatalytic asymmetric hydroarylation of o-hydroxyl styrenes via remote activation of phenylhydrazones, *Tetrahedron: Asymmetry*, **26**, 109 (2015).
8. K. M. Hello, H. H. Mihsen, M. J. Mosa, M. S.r Magtoof, Hydrolysis of cellulose over silica-salicylaldehyde phenylhydrazone catalyst, *J. Taiwan Inst. Chem E.*, **46**, 74 (2015).
9. P. Sudheesh, N. K. Siji, N. K. Chandrasekharan, Third-order nonlinear optical responses in derivatives of phenylhydrazone by Z-scan and optical limiting studies-influence of noble metal nanoparticles, *Opt. Mater.*, **36**, 304 (2013).
10. S. M. Abdel Azeem, S. M. Mohamed Attaf, M. F. El-Shahat, Acetylacetone phenylhydrazone functionalized polyurethane foam: Determination of copper, zinc and manganese in environmental samples and pharmaceutics using flame atomic absorption spectrometry, *React Funct.Polym.*, **73**, 182 (2013).
11. V. K. Gupta, R. N. Goyal, R. A. Sharma, Anion recognition using newly synthesized hydrogen bonding disubstituted phenylhydrazone-based receptors: Poly(vinyl chloride)-based sensor for acetate, *Talanta*, **76**, 859 (2008)
12. Y. Wang, H. Lin, J. Shao, Z. S. Cai, H. K.Lin, A phenylhydrazone-based indole receptor for sensing acetate, *Talanta*, **74**, 1122 (2008).
13. A. Cihaner, F. Alg, A new conducting polymer bearing 4,4-difluoro-4-bora-3a,4a-diaza-s-indacene (BODIPY) subunit: synthesis and characterization.*Electrochim Acta*, **54**, 86(2008).
14. F. Alg, A. Cihaner, An ambipolar low band gap material based on BODIPYand EDOT. *Org. Electron.*, **10**, 450 (2009).
15. F. Yang, S. R. Forrest, Photocurrent generation in nano structured organicsolar cells, *ACS Nano*, **2**, 22 (2008).
16. T. Rousseau, A. Cravino, T. Bura, G. Ulrich, R. Ziessel, J. Roncali, BODIPY derivatives as donor materials for bulk heterojunction solar cells, *Chem. Commun.*,**13**, 1673 (2009).
17. J. A. Duro, G. Torre, J. Barber, J. L. Serrano, T. Torres, Synthesis and liquidcrystal behavior of metal-free and metal-containing phthalocyanines substituted with long-chain amide groups. *Chem. Mater.*, **8**, 1061 (1996).
18. J. H. Olivier, F. Camerel, G. Ulrich, J. Barbera, R. Ziessel, Luminescent ionic liquid crystals from self-assembled BODIPY disulfonate and imidazolium frameworks, *Chem. Eur. J.*, **16**, 7134 (2010).
19. M. Emmelius, G. Pawlowski, H.W. Vollmann, Materials for optical data storage, *Angew. Chem. Int Ed.*, **28**, 1445 (1989).
20. A. Cihaner, F. Alg, Synthesis and properties of 4,4-difluoro-4-bora-3a,4adiaza-s-indacene (BODIPY)-based conducting copolymers. React. Funct. Polym., **69**, 62(2009).
21. J. Zheng, Y. Li, Y. Cui, J. Jia, Q. Ye, L. Han, J. Gao , Isatin-phenylhydrazone dyes and boron complexes with largeStokes shifts: synthesis and solid-state fluorescence characteristics, *Tetrahedron*, **71**, 3802 (2015).
22. Xie, L.; Chen, Y.; Wu, W.; Guo, H.; Zhao, J.; Yu, X. Dyes Pigments, 2012, 92, 1361.
23. G. E. Jara, C. A. Solis, N. S. Gsponer, J. J. Torres, C. A. Glusko, C. M. Previtali, A. B. Pierini, D. M. A. Vera; C. A. Chesta, H. A. Montejano, An experimental and TD-DFT theoretical study on the photophysical properties of Methylene Violet Bernthsen, *Dyes Pigments*, **112**, 341 (2015).
24. H. Li, Z. Chi, X. Zhang, B. Xu, S. Liu; Y. Zhang, J. Xu, New thermally stable aggregation-induced emission enhancement compounds for non-doped red organic light-emitting diodes, *Chem. Commun.* , **47**, 11273 (2011).
25. X. Li, Y. A. Son, Efficient luminescence from easily prepared fluorine–boron core complexes based on benzothiazole and benzoxazole, *Dyes Pigments*, **107**, 182 (2014).
26. Y. H. Chen, J. Z. Zhao, H. M. Guo, L. J. Xi, Geometry relaxation-induced large Stokes shift in red-emitting borondipyrromethenes (BODIPY) and applications in fluorescent thiol probes, *J. Org. Chem.*, **77**, 2192 (2012).